NREL
NATIONAL RENEWABLE ENERGY LABORATORY

Verification of the New FAST v8 Capabilities for the Modeling of Fixed-Bottom Offshore Wind Turbines

Preprint

B. Barahona, J. Jonkman, R. Damiani,
A. Robertson, and G. Hayman
National Renewable Energy Laboratory

To be presented at AIAA SciTech 2015
Kissimmee, Florida
January 5–9, 2015

NREL is a national laboratory of the U.S. Department of Energy
Office of Energy Efficiency & Renewable Energy
Operated by the Alliance for Sustainable Energy, LLC

This report is available at no cost from the National Renewable Energy Laboratory (NREL) at www.nrel.gov/publications.

Conference Paper
NREL/CP-5000-63067
December 2014

Contract No. DE-AC36-08GO28308

This report is available at no cost from the National Renewable Energy Laboratory (NREL) at www.nrel.gov/publications.

Available electronically at http://www.osti.gov/scitech

Available for a processing fee to U.S. Department of Energy and its contractors, in paper, from:

U.S. Department of Energy
Office of Scientific and Technical Information
P.O. Box 62
Oak Ridge, TN 37831-0062
phone: 865.576.8401
fax: 865.576.5728
email: mailto:reports@adonis.osti.gov

Available for sale to the public, in paper, from:

U.S. Department of Commerce
National Technical Information Service
5285 Port Royal Road
Springfield, VA 22161
phone: 800.553.6847
fax: 703.605.6900
email: orders@ntis.fedworld.gov
online ordering: http://www.ntis.gov/help/ordermethods.aspx

Cover Photos: (left to right) photo by Pat Corkery, NREL 16416, photo from SunEdison, NREL 17423, photo by Pat Corkery, NREL 16560, photo by Dennis Schroeder, NREL 17613, photo by Dean Armstrong, NREL 17436, photo by Pat Corkery, NREL 17721.

NREL prints on paper that contains recycled content.

Verification of the New FAST v8 Capabilities for the Modeling of Fixed-Bottom Offshore Wind Turbines

Braulio Barahona*, Jason Jonkman†, Rick Damiani‡, Amy Robertson§, and Greg Hayman¶
National Renewable Energy Laboratory, Golden, CO 80401

Coupled dynamic analysis has an important role in the design of offshore wind turbines because the systems are subject to complex operating conditions from the combined action of waves and wind. The aero-hydro-servo-elastic tool FAST v8 is framed in a novel modularization scheme that facilitates such analysis. Here, we present the verification of new capabilities of FAST v8 to model fixed-bottom offshore wind turbines. We analyze a series of load cases with both wind and wave loads and compare the results against those from the previous international code comparison projects–the International Energy Agency (IEA) Wind Task 23 Subtask 2 Offshore Code Comparison Collaboration (OC3) and the IEA Wind Task 30 OC3 Continued (OC4) projects. The verification is performed using the NREL 5-MW reference turbine supported by monopile, tripod, and jacket substructures. The substructure structural-dynamics models are built within the new SubDyn module of FAST v8, which uses a linear finite-element beam model with Craig-Bampton dynamic system reduction. This allows the modal properties of the substructure to be synthesized and coupled to hydrodynamic loads and tower dynamics. The hydrodynamic loads are calculated using a new strip theory approach for multimember substructures in the updated HydroDyn module of FAST v8. These modules are linked to the rest of FAST through the new coupling scheme involving mapping between module-independent spatial discretizations and a numerically rigorous implicit solver. The results show that the new structural dynamics, hydrodynamics, and coupled solutions compare well to the results from the previous code comparison projects.

I. Introduction: FAST Modularization Framework

Given the challenging environmental conditions of offshore wind energy and the need to reduce costs, accurate modeling of the dynamic response of offshore wind turbines is fundamental to improving their design. Therefore, wind turbine computer-aided engineering (CAE) tools need to take a system approach for predicting aerodynamic and hydrodynamic loads throughout the support structure, rotor, and drive train components. Large international code comparison efforts[1–3] have helped to push forward the development of such CAE tools (i.e., wind turbine design codes). In this context, the aero-hydro-servo-elastic tool FAST[4], developed at the National Renewable Energy Laboratory (NREL), has been reformulated to enhance its development flexibility and capabilities to model multiple physics domains with different levels of fidelity. The novel FAST v8 consists of a modularization framework described in detail in Refs. 5 and 6. The framework contains modules for aerodynamics (AeroDyn); hydrodynamics (HydroDyn); control and electrical drive dynamics (ServoDyn); rotor, drivetrain, nacelle, tower, and platform structural dynamics (ElastoDyn); multimember substructure structural dynamics (SubDyn); mooring statics and dynamics (MAP); and ice loads (IceFloe). A new nonlinear finite-element structural dynamics module (BeamDyn) for blades, a finite-element module for mooring dynamics (FEAMooring), and a module for advanced ice loads (IceDyn) are also under development. Fig. 1 shows the difference in architecture between FAST v7 and FAST v8.

In the FAST v8 framework, a *driver code* handles the time and spatial coupling across the modules. Key features of this coupling include a new mesh-to-mesh mapping scheme between module-independent spatial discretizations and a numerically rigorous input/output solve for implicit coupling[7].

SubDyn[8] uses a linear finite-element beam method and Craig-Bampton reduction with static improvement. A detailed description and a work flow describing the integration of SubDyn in FAST v8 can be found in Refs. 8 and 9. Substructures modeled in SubDyn can be composed of Euler-Bernoulli or Timoshenko beam elements. Timoshenko beam elements include shear deflection and are therefore appropriate for modeling structures with members that are

*Postdoctoral researcher, National Wind Technology Center, 15013 Denver West Parkway, Golden, CO 80401, braulio.barahonagarzon@nrel.gov
†Senior Engineer, National Wind Technology Center, 15013 Denver West Parkway, Golden, CO 80401, AIAA Professional Member.
‡Senior Engineer, National Wind Technology Center, 15013 Denver West Parkway, Golden, CO 80401, AIAA Professional Member.
§Senior Engineer, National Wind Technology Center, 15013 Denver West Parkway, Golden, CO 80401
¶Senior Engineer, National Wind Technology Center, 15013 Denver West Parkway, Golden, CO 80401

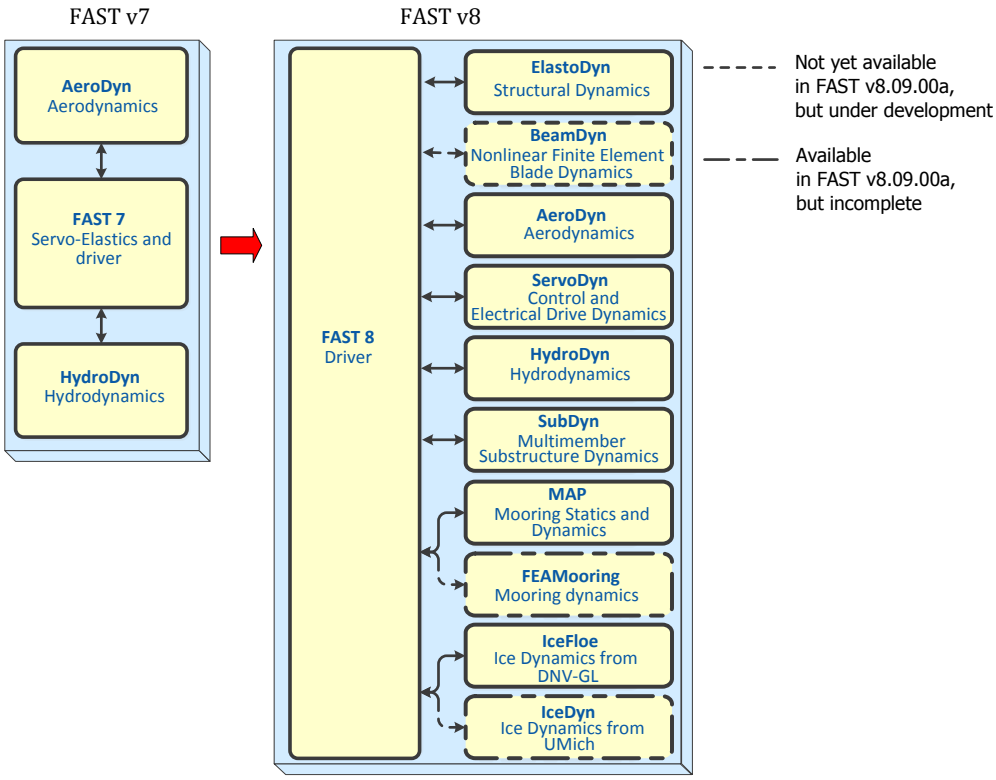

Figure 1. Illustration of the differences in the architecture of FAST v7 and the new FAST v8 modularization framework, taken from Ref. 6.

not slender and/or are interconnected in a multimember structure. The choice of a linear finite-element model is considered appropriate because substructures in general are very stiff and geometric nonlinear effects have relatively little influence in terms of loads and displacements at the base of the tower[10]. SubDyn can be run in stand-alone mode to analyze modes and static response of substructures only. When coupled to FAST v8, a SubDyn model can be reduced to a specified number of modes using the Craig-Bampton reduction method, with the higher modes treated quasi-statically, and formulated in state space[8]. The number of modes kept will dictate the frequency bandwidth of the coupled model; in general, higher modes do not contribute to the overall dynamic response. In addition, when modes with high frequencies are kept, the system becomes numerically stiff and implicit solutions or very small time steps would be necessary. Other considerations regarding the current version of SubDyn are (1) the substructure is clamped to the seabed, and rigidly connected to the base of the tower in ElastoDyn; (2) self weight is applied at each node as a distributed load; (3) other loads and mass/inertia properties such as those from marine growth and flooding/ballasting are calculated in HydroDyn; (4) tapered members are implemented as cylinders with stepwise variations of their properties.

On the hydrodynamic side, HydroDyn[11,12] is now extended to compute hydrodynamic loads on multimember substructures, including strip theory using an extended Morison's formulation (taking into account fluid inertia, added mass, and viscous loads, including relative velocity effects based on the undisturbed wave kinematics); buoyancy; flooded members; marine growth; tapered members; and end effects. HydroDyn treats waves using first-order (Airy) or first- plus second-order wave theory, with the option to include directional spreading. No wave stretching or higher order wave theories are included, however.

To couple hydrodynamic loads to the substructure structural dynamics, the new mesh-mapping capabilities of FAST v8[7] transfer motions and loads back and forth, between the structure and the hydrodynamics calculations, allowing SubDyn, HydroDyn, and ElastoDyn to have independent spatial discretizations appropriate to their respective needs. In particular, motions of the transition piece (including accelerations) are passed from ElastoDyn to SubDyn; motions across the substructure (including accelerations) are passed from SubDyn to HydroDyn; hydrodynamic loads (including acceleration-dependent added-mass loads) are passed from HydroDyn to SubDyn; and substructure reaction loads (including acceleration-dependent reactions) at the transition piece are passed from SubDyn to ElastoDyn. The acceleration-dependent terms mean that the coupling relations are implicit. The verification work we present here

demonstrates that this coupling scheme yields consistent and reliable results.

In the following sections, we describe the substructure models and load cases used for the verification. Results from three different systems (monopile, tripod, and jacket) are presented. In the last section, we give a summary and outlook for future work.

II. Fixed-Bottom Offshore Wind Turbine Models and Verification Objectives

The wind turbine model used for this verification is the baseline 5-MW NREL wind turbine[13] with three different fixed-bottom offshore support structures. First, we use a monopile substructure (Subsection A) as a reference to ensure consistency between FAST v8 and the previous version, FAST v7, in which it was possible to model monopiles. From the load cases specified in Phase I of the Offshore Code Comparison Collaboration (OC3[a]), we selected a few to verify our results. Then, we modeled two multimember substructures in FAST v8: a tripod and a jacket (Subsection B). Next, we verified the results of the tripod model against those from Phase III of the OC3, and verified the jacket model results against Phase I of the Offshore Code Comparison Collaboration Continuation (OC4[b]). The wind turbine rotor and controls are the same for the three support structures.

A. Monopile Substructure

This type of substructure is used for shallow water depths, typically less than 30 m. In Phase I of OC3[1,14], the monopile sits on the seabed with a rigid foundation in 20-m water depth and extends 10 m above the mean sea level (MSL) where it couples to the base of the tower. The model of the monopile substructure in SubDyn is illustrated in Fig. 2. It consists of four joints (in maroon). Joint 1 is a rigid boundary located at the seabed (i.e., mud-line), and joint 4 is the interface that exchanges loads and motions with ElastoDyn. Each set of two joints defines a member, which is further discretized into three 3.333-m-long elements. Similarly, the HydroDyn model consists of one member, defined by joints 1 and 2 (in blue). As indicated in Fig. 2, the member is refined with nodes spaced 0.5 m from each other. Hydrodynamic loads calculated per unit length by HydroDyn along its members are mapped to the corresponding SubDyn nodes and imposed as lumped loads. It is noted that the HydroDyn and SubDyn discretizations need not have the same resolution.

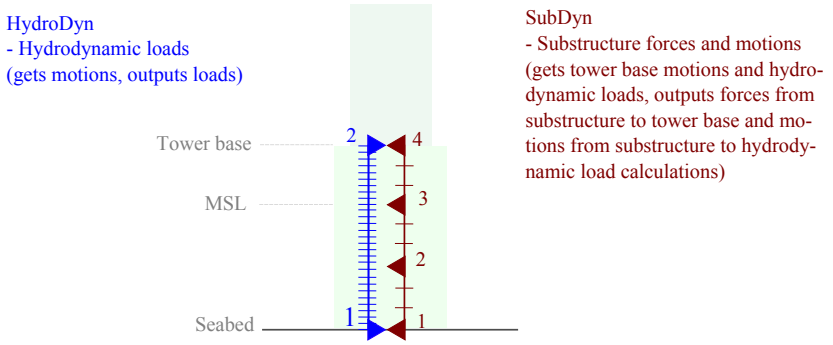

Figure 2. Illustration of the monopile model in FAST v8 —SubDyn and HydroDyn.

Table 1 describes the load cases we analyzed for the monopile model. They are a subset of those in Refs. 1 and 14. They all model the complete wind turbine on a monopile substructure, but in Cases 4.1 and 4.2 only the tower and substructure are flexible (therefore modeling a sort of *inverted pendulum*) and wind loads are not considered, the objective is to focus on the response of the system to hydrodynamic loads. Cases 5.1 to 5.3 consider a fully flexible turbine under combined wind and wave loads. Turbulent wind fields for the stochastic simulations were created[14] with the Mann model and power law for wind shear according to the relevant standards. Regular waves are specified with linear (i.e., Airy) wave theory and linear irregular waves are specified with Pierson-Moskowitz spectrum. Regular waves are defined by a wave height H and a wave fundamental frequency period T. The linear irregular waves are a composition of regular waves with a given significant wave height H_s and peak-spectral period T_P. In addition, Wheeler stretching method is specified[14] to correct (i.e., to stretch) the wave kinematics above the MSL to the instantaneous free surface of the water.

[a]The OC3 was an international benchmark of aeroelastic codes under International Energy Agency (IEA) Wind Task 23 – Subtask 2. It took place from 2004 to 2009.

[b]The OC4 was a continuation of OC3, under IEA Wind Task 30. This project finished in 2013.

Table 1. Subset of OC3 Phase I load cases and environmental conditions

Load case	Flexible subsystems	Wind conditions	Wave conditions	Simulation length (s)	Initial rotor speed (rpm)
4.1	Substructure, tower	None: ρ_{air} = 0 kg/m^3	Regular: H = 6 m, T = 10 s	60	0
4.2	Substructure, tower	None: ρ_{air} = 0 kg/m^3	Irregular: H_s = 6 m, T_P = 10 s	600	0
5.1	All	Steady: V_{hub} = 8 m/s	Regular: H = 6 m, T = 10 s	60	9
5.2	All	Stochastic: V_{hub} = 11.4 m/s, I_{ref} = 0.14	Irregular: H_s = 6 m, T_P = 10 s	600	12
5.3	All	Stochastic: V_{hub} = 18 m/s, I_{ref} = 0.14	Irregular: H_s = 6 m, T_P = 10 s	600	12

B. Multimember Substructures

Multimember substructures are typically used in transitional-depth waters 30 to 60 m deep, which are deeper than those suitable for monopiles or gravity-based foundations. They are essentially lattice-like or welded tubular steel frames, where many of the members may connect to the same joint, be oriented at different angles, or be significantly tapered. Fig. 3 illustrates the geometry of the two multimember substructures that we analyzed, the OC3 tripod, and the OC4 jacket. The members and joints/nodes where sensors are located to verify the responses computed by FAST v8 are highlighted. The tripod is situated at 45-m water depth. The details of the geometry and the properties can be found in Refs. 2, 14, and 15. Similarly, the jacket substructure is at 50-m water depth. Details can be found in Ref. 16.

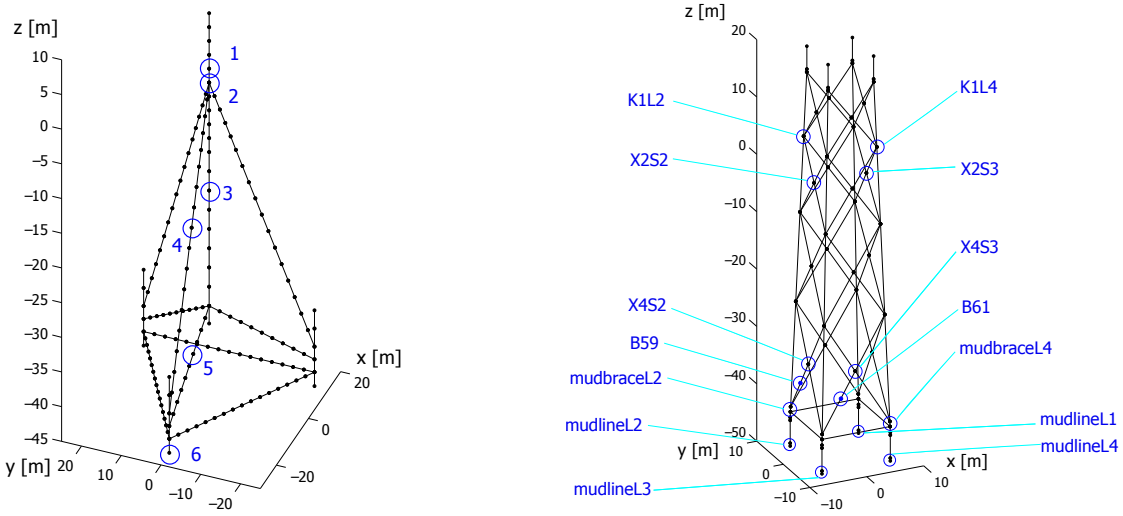

a) Tripod structure from OC3. The numbers indicate the locations of sensors

b) Jacket structure from OC4. Labels indicate the locations of sensors

Figure 3. Illustration of tripod and jacket models in SubDyn.

The tripod was studied in Phase III of the OC3 project; as a result, the simulation cases stem from those in Phase I (monopile). Some cases, which focused on the turbine response, did not need to be rerun because the models are identical. In addition, cases to verify static loads resulting from gravity and buoyancy were added[14]. Table 2 describes the load cases we analyzed. They are practically the same as cases 4.3 and 5.1 of the monopile but with shorter simulation times and larger wave heights. Note that in these cases a Stream function (Dean) was prescribed;[14,15] however, the FAST v8 results are computed with either linear Airy waves or second-order regular waves (based on Stokes theory). We did not compute wave kinematics at the instantaneous free surface of the sea for either case. The

full set of cases from the OC3 project Phase III can be found in Ref. 14.

Table 2. Subset of OC3 Phase III load cases and environmental conditions

Load case	Flexible subsystems	Wind conditions	Wave conditions	Simulation length (s)	Initial rotor speed (rpm)
4.3	Substructure, tower	None: ρ_{air} = 0 kg/m^3	Regular: H = 8 m, T = 10 s	30	0
5.1	All	Steady: V_{hub} = 8 m/s	Regular: H = 8 m, T = 10 s	30	9

Similarly, the subset of load cases (from those defined in Phase I of the OC4 project[16]) that we analyzed for the jacket substructure are described in Table 3. Turbulent wind fields for the stochastic simulations are based on the Normal Turbulence Model and power law for wind shear. Ref. 16 specifies linear regular Airy waves and linear irregular waves with Wheeler stretching method. We computed the FAST v8 results for the regular wave case with linear Airy waves and with second-order regular waves based on Stokes theory, but without using a stretching method to compute the wave kinematics at the instantaneous free surface of the sea. Reference 16 specifies the inertia coefficient $c_m = 2$ and the drag coefficient $c_d = 1$. All the simulations consider a layer of 0.1 m of marine growth with a density of 1100 kg/m^3 on all the members of the substructure below 2 m of the MSL and down to 40-m depth. The subset of load cases selected include stochastic and deterministic cases. The stochastic cases use only one seed, but have a long duration of 3600 s to make them statistically comparable.

Table 3. Subset of OC4 load cases and environmental conditions

Load case	Flexible subsystems	Wind conditions	Wave conditions	Simulation length (s)	Initial rotor speed (rpm)
4.3b	Substructure, tower	None: ρ_{air} = 0 kg/m^3	Regular: H = 8 m, T = 10 s	30	0
4.5	Substructure, tower	None: ρ_{air} = 0 kg/m^3	Irregular: H_s = 6 m, T_P = 10 s	3600	0
5.6	All	Steady: V_{hub} = 8 m/s	Regular: H = 8 m, T = 10 s	30	9
5.7	All	Stochastic: V_{hub} = 18 m/s, I_{ref*}=0.14	Irregular: H_s = 6 m, T_P = 10 s	3600	12.1

III. Code Comparison Results

For this verification project, we thoroughly analyzed a subset of load cases for each configuration to verify the capabilities of FAST v8. Those cases are described in Tables 1 to 3, for the monopile, tripod, and jacket, respectively. For all cases, wind and waves are aligned and the rotor is oriented upwind with no yaw error. The transients at the beginning of the simulation are removed and the position of the rotor blades is kept consistent with the specified initial conditions. In this section, we present representative results of the structure's dynamic response to demonstrate the new modeling capabilities of FAST v8 and verify them with the work performed in the OC3[1,2] and the OC4[3] projects. The results we present exemplify the dynamics that are consistent with other codes and also point out those in which modeling differences yield different results.

A. Coupled Simulation Setup

Here we summarize the main simulation setup related to the coupled hydro-elastic model. We describe the main settings of the driver code that handles the coupling across the modules in the new FAST v8 framework and the relevant settings of SubDyn for the coupling to the FAST v8 framework. These are important settings to guarantee numerical stability, reduce simulation time, and increase accuracy. Table 4 shows the values of global time step `dt`, the order of the interpolation/extrapolation (`InterpOrder`) of the inputs to each module, and the number of corrections (`NumCrctn`) of the predictor–corrector coupling method, all of which are set in the main input file (i.e., `*.fst`). `dt` should be chosen small enough compared to the highest natural frequency f_{max} of the coupled model. The rule of thumb in Ref. 6 is that `dt` should be ten times smaller than $1/f_{max}$. `NumCrctn` can be set to zero (no corrections) or to a positive integer. As long as `dt` is small enough, the solution of the models can be stable without any corrections.

Including corrections may be necessary, though, to achieve a given convergence rate of an underlying time integrator. `InterpOrder` can be set to linear (1) or quadratic (2) interpolation/extrapolation.

Table 4. Coupling and time integration simulation settings

	DT (s)	InterpOrder	NumCrctn	NDiv	NModes	MDivSize (m)
Monopile	0.005	2	0	3	0	0.5
Tripod	0.008	2	1	1	12	1
Jacket	0.01	2	1	2	8	1

In addition, the number of divisions (`NDiv`) for each member of the substructure modeled in SubDyn and the number of Craig-Bampton modes retained (`NModes`) are shown in Table 4 for each model. `NDiv` will ultimately define the resolution of the substructure because the length of each member will be divided by `NDiv`. For example, the monopile model (Fig. 2) has 10-m-long members, divided into 3.333-m-long elements. In the case of the tripod, elements are approximately between 2 m and 3 m; and for the jacket, the largest elements are approximately 6.6 m long. Such element lengths aim at keeping high enough resolution in the substructure model to match that specified in HydroDyn for the calculation of hydrodynamic loads. The resolution in HydroDyn is set by defining the maximum spacing between nodes (`MDivSize`). This allows us to minimize the inherent error of mapping from the distributed hydrodynamic loads to the point loads applied at the substructure nodes.

`NModes` was selected to keep all Craig-Bampton modes up to 10 Hz. We consider that keeping this bandwidth is sufficient because wind and wave excitation drop dramatically above 4 Hz.

The integration method used in SubDyn was the explicit Adams-Bashforth-Moulton (ABM4) method; the Static-Improvement Method implemented in SubDyn is used to account for buoyancy and gravity while selecting only the lower Craig-Bampton modes; Timoshenko beam elements are used in the finite-element formulations. In addition, we added damping at the tower base in the heave direction to avoid spurious oscillations in the heave degree of freedom (DOF), observed when simulating the impulse response of the system. The damping was added via HydroDyn's additional linear damping matrix and is of the order of 1 MN/(m/s) for a damping ratio of 1% of critical damping.

The input files of these models can be downloaded from Ref. 6 with the latest FAST v8 release, they correspond to `Test19.fst`, `Test20.fst`, and `Test21.fst`, for the monopile, tripod, and jacket, respectively.

B. Monopile Results

The monopile is a first step in the verification, because the model is relatively simple (Fig. 2) and it can also be modeled in FAST v7. The results from the OC3 project using FAST v7 can therefore be used to check the solution of FAST v8. In general, we observed a good agreement between FAST v7 and FAST v8, with some differences caused by the limitations of the modeling approach in FAST v7. In Fig. 4, for example, where the global dynamics of the rotor nacelle assembly are summarized for case 5.1 (Table 1, steady wind and regular waves), minor differences can be observed in the mean value and phase of tower-top fore-aft displacement (`TTDspFA`[c], Fig. 4c). The reason for this is that FAST v7 models the monopile as an extension of the tower, with two global fore-aft and two side-to-side modes. FAST v8, though, uses SubDyn to model the monopile and ElastoDyn for the tower. The finite-element model in SubDyn is then reduced to the desired number of modes. The result is a slightly different fore-aft natural frequency of the substructure and tower. If desirable, the tower modes could be modified by changing the stiffness and damping in FAST model. The difference in the phase of the tower-top fore-aft displacement could be adjusted using the stiffness tuning factors to modify the frequency, at the expense of a different mean value of the displacement.

In any case, the loads and deflections of the wind turbine rotor are essentially the same, as shown by the out-of-plane tip deflection (`OoPDefl1`, Fig. 4a) and root flap-wise bending moment (`RootMyc1`, Fig. 4b) of blade one. We can also see that FAST v8 results are very similar to the results from the majority of the other participants in the OC3 project, which are labeled *Other* in Figs. 4 to 6.

In addition, FAST v8 can model the response at the transition piece between the tower and the substructure. For the monopile model, this is the interface of the tower base (modeled in ElastoDyn) and the monopile (modeled in SubDyn); which corresponds to joint 4 in SubDyn as illustrated in Fig. 2. This was not possible to model with FAST v7.

In the case of steady wind and regular waves (case 5.1 in Table 1), the fore-aft motion of the transition piece (`PtfmSurge`) measured at the tower base, follows the periodicity of the wave loads. As illustrated in Fig. 5a, FAST

[c]Throughout this paper the FAST v8 output channels names are printed in the y-axis of the plots together with the corresponding units.

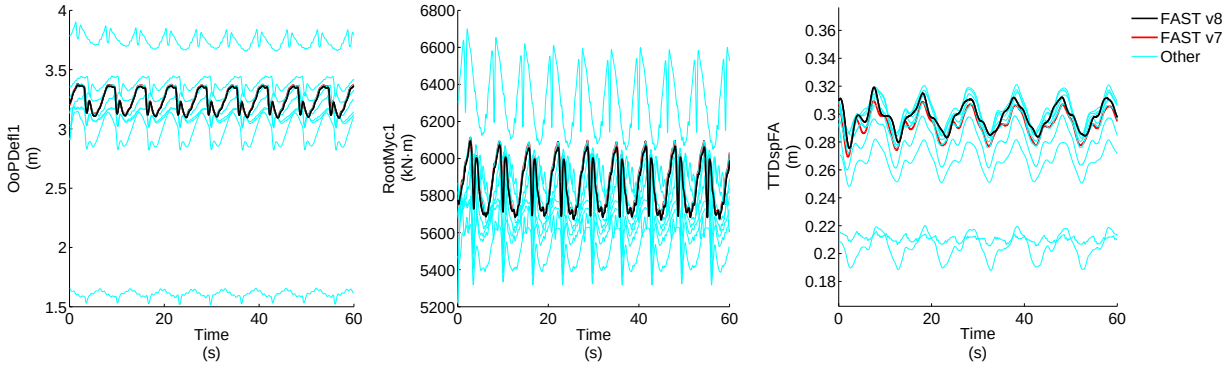

a) Out-of-plane blade-tip deflection **b) Blade-root flap-wise bending moment** **c) Tower-top fore-aft displacement**

Figure 4. Monopile: OC3 case 5.1, steady wind and regular waves.

v8 shows the expected periodicity of this fore-aft (i.e., surge) motion, which matches quite well with the majority of results computed by other codes. We also illustrate this with stochastic simulations, shown in Figs. 5b and 5c, which show that the frequencies are well predicted for the fore-aft motion and the statistics of the signal are similar to others from the OC3 benchmark exercise.

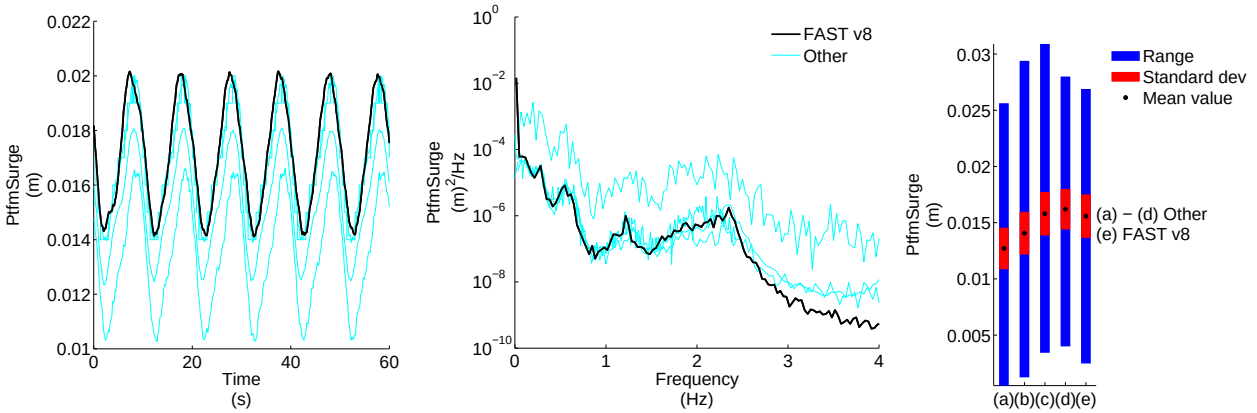

a) OC3 case 5.1, steady wind and regular waves **b) OC3 case 5.3, turbulent wind (mean wind speed above rated) and irregular waves** **c) OC3 case 5.3, turbulent wind (mean wind speed above rated) and irregular waves**

Figure 5. Monopile: fore-aft motion of transition piece measured at tower base.

To finalize the verification of the monopile, Figs. 6a and 6b show the expected periodicity of the fore-aft moment (`ReactMYss`) and shear force (`ReactFXss`) calculated by SubDyn caused by the forcing of regular waves. FAST v8 compares well with the results from the participants in the OC3 project (including FAST v7). Differences can be observed mainly in the minimum value of the fore-aft moment. This may be related to the wave forcing, because HydroDyn in FAST v8 does not yet include stretching of the wave kinematics to the instantaneous free surface of the sea.

As we move up the substructure, the mean value and range of the fore-aft moment reduces and the periodicity of the waves is less accentuated, as shown by the fore-aft moment at the MSL in Fig. 6c (`M2N1MKye`).

C. Multimember Substructure Results

1. Tripod Results

This section contains the results of the FAST v8 tripod model compared to those from OC3 Phase III. Some differences are expected, mainly related to the wave kinematics input and the buoyancy calculation. For example, Fig. 7a shows HydroDyn's regular Airy wave elevation output (`Wave1Elev` in black), which differs slightly from the specified

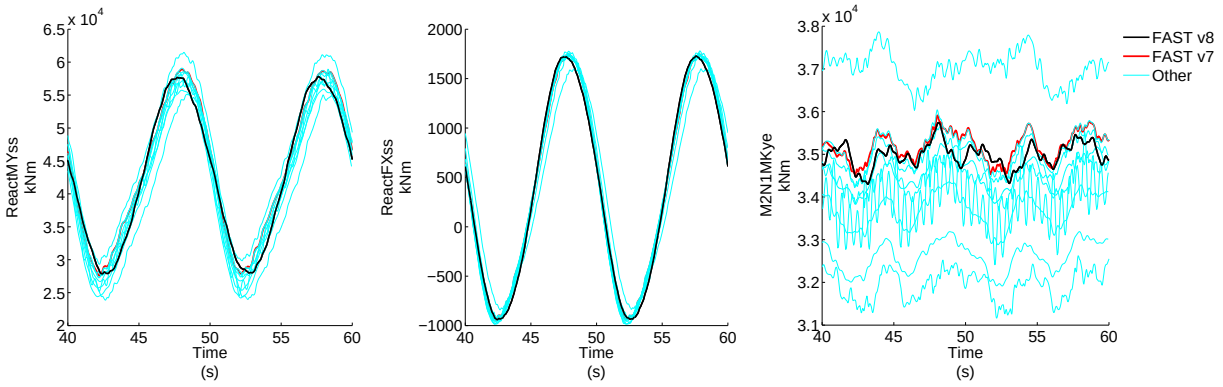

a) Fore-aft moment at seabed **b) Fore-aft shear force at seabed** **c) Fore-aft moment at MSL**

Figure 6. Monopile: OC3 case 5.1, steady wind and regular waves.

regular wave with Dean Stream function calculated by other codes. HydroDyn's regular Airy waves are sinusoidal. The Dean stream function produces a narrower and taller crest—in both cases the mean value of the wave is zero. HydroDyn's new capability to produce second-order waves captures many of the characteristics of the Dean stream function, as the results in Fig. 7a show. HydroDyn's second-order waves fit very well with most of the output from other codes.

Despite the improvement in the wave kinematics, there is practically no impact on the overall dynamics of the wind turbine and support structure, indicating that the differences are more the result of solving the wave kinematics to the instantaneous free surface than the result of higher order potentials. This is shown by the substructure fore-aft displacement (`M1N1TDxss`) and pitch fore-aft rotation at MSL (`M1N1RDye`), along with the tower-top fore-aft displacement (`TwHt1TPxi`) calculated by FAST v8. These results are shown in Figs. 7b to 7d for the regular Airy waves and for the second-order waves.

In terms of global dynamics, there are clear differences between FAST v8 and the other codes. These may be attributed to several modeling differences, such as wave kinematics. For example, the main oscillation patterns in the fore-aft displacement (`M1N1TDxss`) and rotation of the substructure (`M1N1RDye`) at MSL, computed by FAST v8 are similar to those from the other codes, but with less pronounced higher order effects. In the tower-top displacements there is a wide spread in the results from the different codes. The FAST v8 results show generally smaller amplitudes.

Regarding the loads, an aspect that seems to bring differences in the response is the resolution of wave kinematics up to the instantaneous free surface of the sea. We infer this from Fig. 8, where forces and moments 2 m above MSL and at MSL are shown. The fore-aft shear loads on the top plots—computed by the other codes—include a component with the same period as the wave and with a significantly larger amplitude. Looking at the fore-aft bending moments on the bottom plots, we can see phase and amplitude differences across the different codes. Generally, the output of FAST v8 shows smaller amplitude.

As we move down the structure to the legs and the braces, the axial forces start to dominate the loads on the substructure. This is illustrated in Fig. 9 where the axial force on the upwind leg (`M3N1FKze` in Fig. 9c; its location is indicated by sensor 4 in Fig. 3a) is shown to be many orders of magnitude larger than the shear forces. All the codes show axial force with very similar periods, but there are visible differences in the amplitude and mean value. The shear force perpendicular to the wave direction is practically zero and the one influenced by gravity and buoyancy (i.e., `M3N1FKye` in Fig. 9b) is two orders of magnitude smaller than the axial force (`M3N1FKze`). In this case, FAST v8 predicts loads with a different mean value than the other codes. The most likely reason for this is that the volume of the substructure is overestimated because the overlapping of members at the joints is not taken into account as it is in the other codes. This gives a larger buoyancy force that makes the mean value of the shear force (`M3N1FKye`) smaller. Similarly, the bending moment about the axis perpendicular to the wave direction (`M3N1MKxe` in Fig. 9a) is the most significant, and most of the codes show a fairly similar response. The bending moments about the other axes (i.e., lateral bending moment [`M3N1MKye`] and torsion moment [`M3N1MKze`]), are practically zero. We observe the same behavior on forces and moments in the downwind legs and in the braces.

Finally, forces and moments at the piles that fix the structure to the seabed are reported here. The response on the upwind pile in terms of the relevant loads is shown in Fig. 10. In this case, because the piles are vertical, the fore-aft shear force (`M9N1FKxe` in Fig. 10b) and axial force (`M9N1FKze` in Fig. 10c) are the main forces, and there is a rough

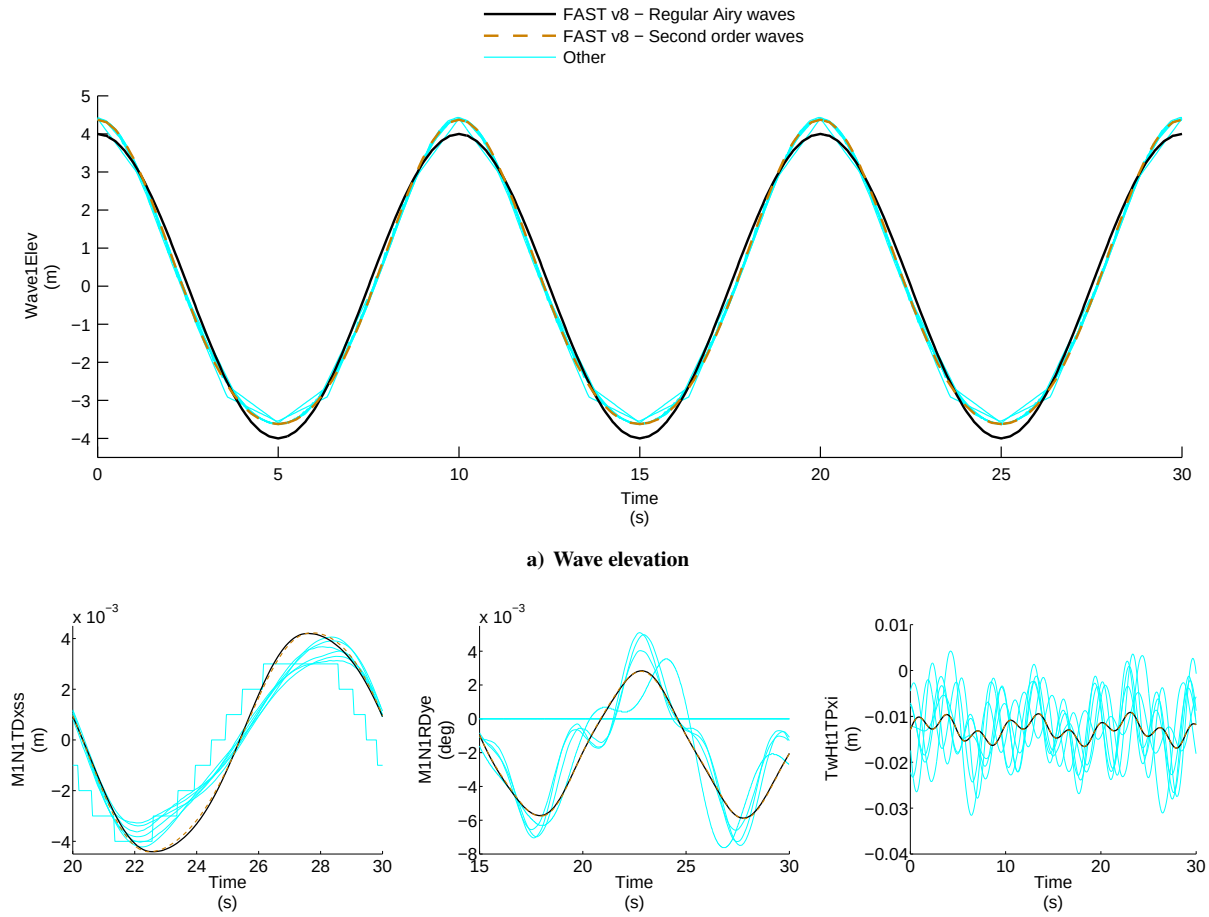

a) Wave elevation

b) Substructure fore-aft displacement at MSL

c) Substructure fore-aft pitch at MSL

d) Tower-top fore-aft displacement

Figure 7. Tripod: OC3 case 4.3, regular waves and no wind.

agreement among the codes. The fore-aft bending moment (`M9N1MKye` in Fig. 10a) also dominates and all the codes show similar responses with a small difference in phase and period and more noticeable differences in the amplitude. The same observations are valid for the downwind piles.

The previous observations for case 4.3 generally hold for case 5.1. For some of the outputs, however, there is a larger spread among the different codes in mean, maximum, and minimum values. For example, as illustrated in Fig. 11, fore-aft shear force (`M1N2FKxe`) and bending moment at the tower base (`M1N1MKye`), as well as the tower-top fore-aft displacement (`TwHt1TPxi`) show some large differences.

2. *Jacket Results*

The OC4 jacket is illustrated in Fig. 3b, and the subset of cases analyzed in this work is described in Table 3. The analysis included 58 sensors distributed across the wind turbine from the rotor to the substructure. Generally, the same observations are valid as with the tripod substructure. The main difference is that the shear forces in the members of the jacket are less influenced by buoyancy. This is because the jacket members are more homogeneous and the main frame (i.e., the legs) is practically vertical.

We used regular wave kinematics with second-order terms, to better represent waves from strip theory as it was shown by the wave elevation in Fig. 7. Rotor blade root forces and deflections (as well as those measured at the middle of the blade), loads on the yaw bearing, and global dynamics of the tower and substructure show similar dynamics among the different codes, up to around 3 Hz.

In the rest of this section we present selected results of case 4.3b and case 5.7 to illustrate the response of the jacket. Figs. 12a to 12c show forces and overturning moment at the base of the jacket at the seabed. The force on the global z-axis (`-ReactFZss`) agrees very well with the other codes. The shear force (`ReactFXss`) and overturning moment

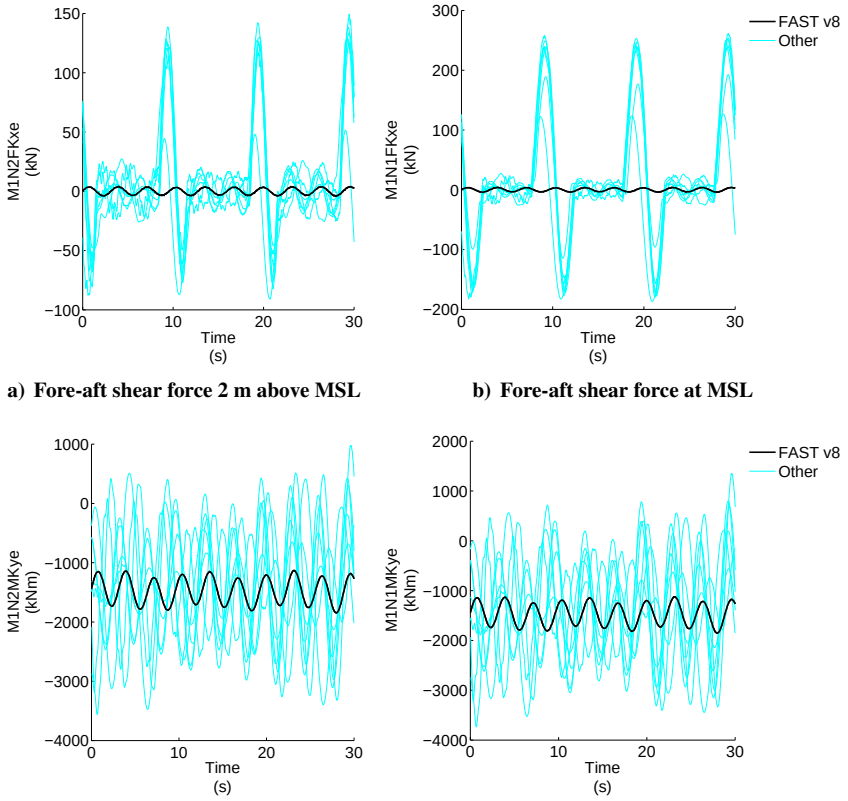

a) Fore-aft shear force 2 m above MSL

b) Fore-aft shear force at MSL

c) Fore-aft bending moment 2 m above MSL

d) Fore-aft bending moment at MSL

Figure 8. Tripod: OC3 case 4.3, regular waves (second-order) and no wind (sensors 1 and 2 in Fig. 3a).

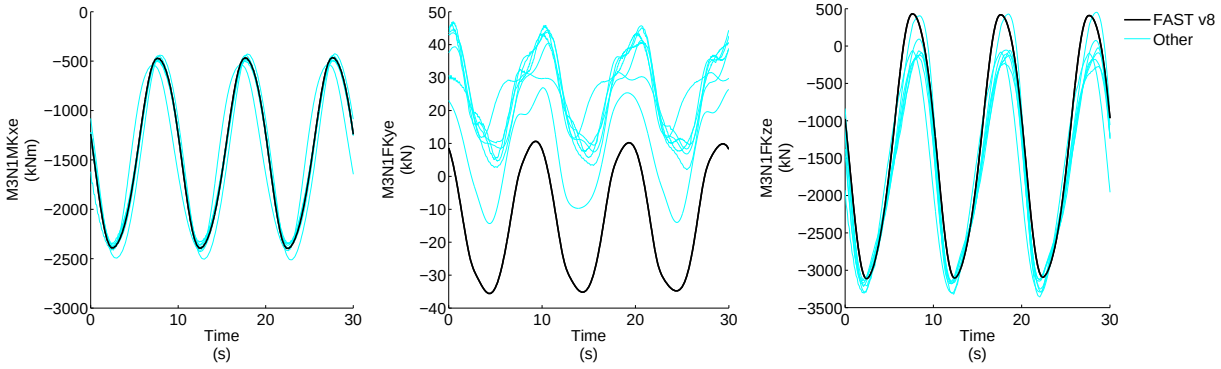

a) Bending moment

b) Shear force

c) Axial force

Figure 9. Tripod: OC3 case 4.3, regular waves (second-order) and no wind (sensor located on upwind leg, 4 in Fig. 3a).

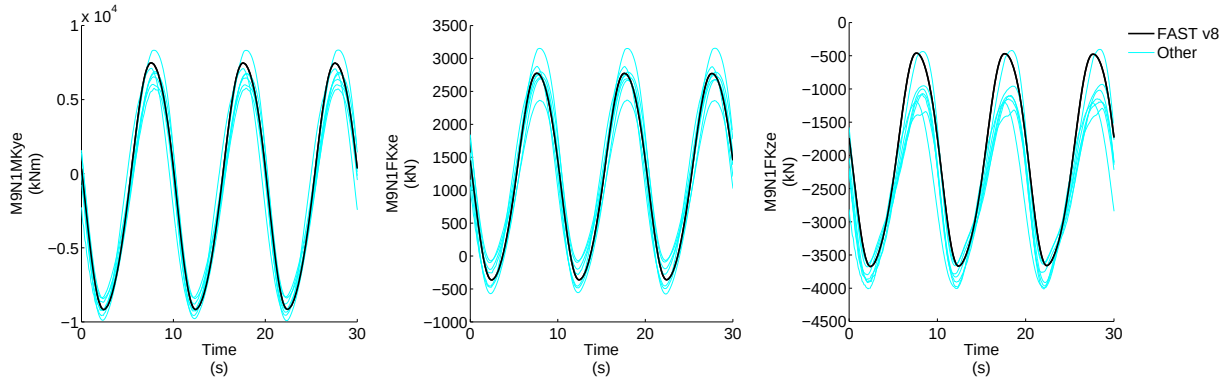

a) Bending moment b) Shear force c) Axial force

Figure 10. Tripod: OC3 case 4.3, regular waves (second-order) and no wind (sensor located on upwind pile at seabed, 6 in Fig. 3a).

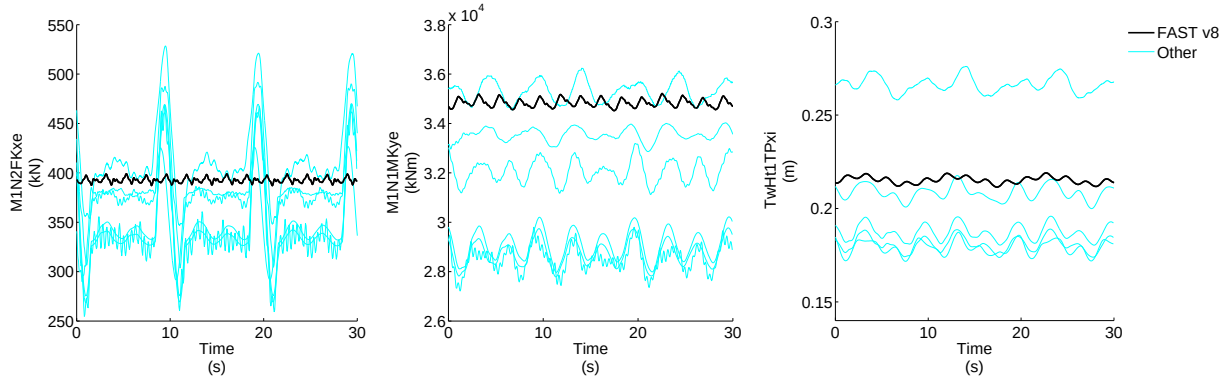

a) Fore-aft shear force 2 m above MSL b) Fore-aft bending moment at MSL c) Tower-top displacement

Figure 11. Tripod: OC3 case 5.1, regular waves (second-order) and no wind.

(ReactMYss) show very similar responses to the majority of the codes with slightly smaller amplitude. Out-of-plane deflections at different levels on the front side (i.e., the side upwind and perpendicular to the main wind direction, side 2) of the jacket also generally agree with other codes. The differences are that FAST v8 results show smaller maximum–minimum values and less visible higher frequency content. Fig. 12d shows the out-of-plane deflection at the center of one of the X-joints at the upper part (M3N1TDXss, corresponding to sensor X2S2 in Fig. 3b) of the jacket. Fig. 12e shows the same measurement farther down the structure (M5N2TDXss, corresponding to sensor X4S2).

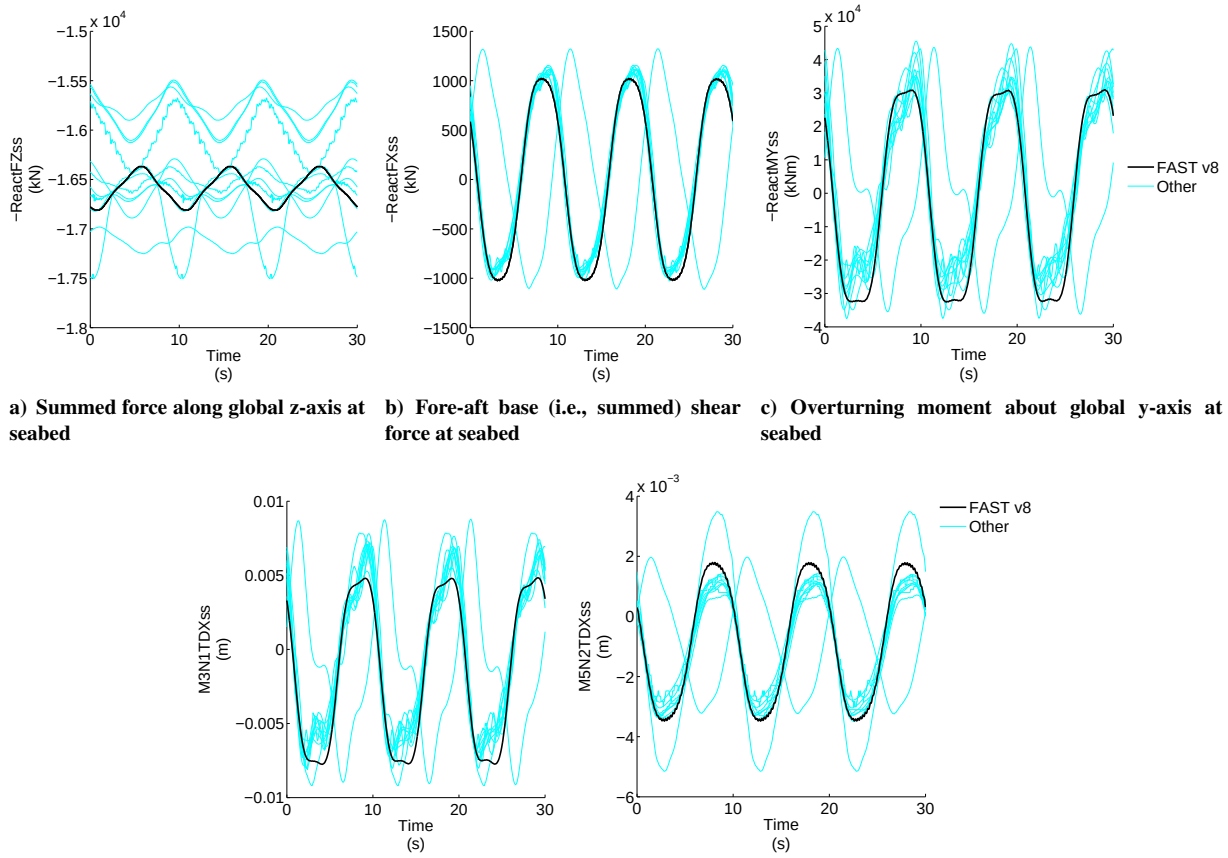

a) Summed force along global z-axis at seabed

b) Fore-aft base (i.e., summed) shear force at seabed

c) Overturning moment about global y-axis at seabed

d) Out-of-plane deflection at center of X-joint at level 2 on side 2

e) Out-of-plane deflection at center of X-joint at level 4 on side 2

Figure 12. Jacket: OC4 case 4.3b, regular waves and no wind.

Case 5.7 in Phase I of the OC4 project consisted of irregular waves and turbulent wind as described in Table 3. Fig. 13 shows the power spectral density of the flapwise bending moment at the wind turbine rotor blade 1 (Spn2MLyb1), shear force at the yaw bearing (YawBrFxp), and shear force at the base (ReactFXss). Lower frequencies agree to some extent across most of the different codes. Out-of-plane deflection and forces on the front side of the jacket are shown in Fig. 14.

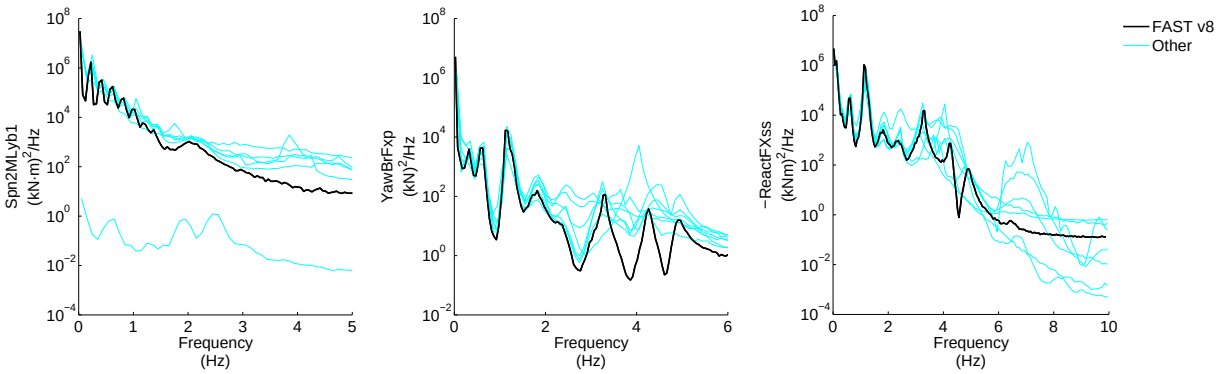

a) Blade 1 flapwise bending moment at 50% span **b) Tower-top fore-aft shear force** **c) Fore-aft base shear force**

Figure 13. Jacket: OC4 case 5.7, irregular waves and turbulent wind.

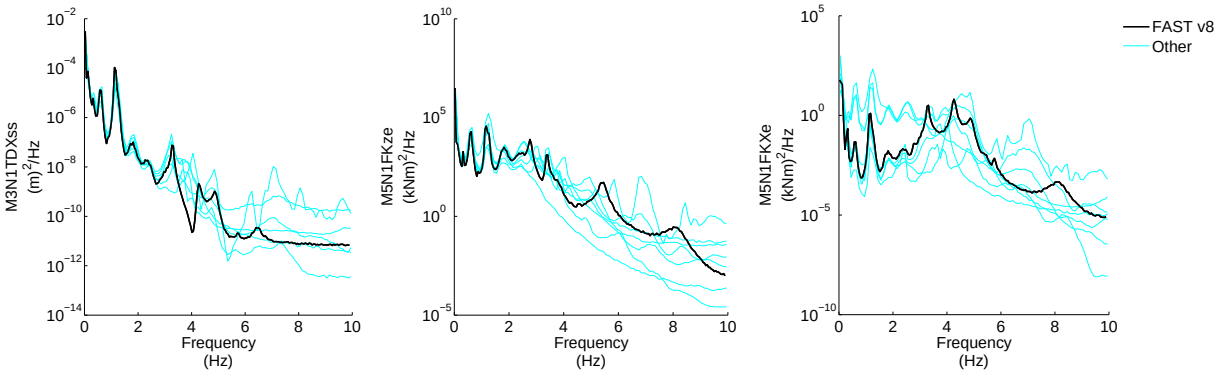

a) Out-of-plane deflection at center of X-joint at level 2 on side 2 **b) Axial force in the center of brace 59** **c) Out-of-plane shear force in the center of brace 59 (located at level 4 on side 2)**

Figure 14. Jacket: OC4 case 5.7, irregular waves and turbulent wind.

IV. Summary and Future Work

The FAST v8 modularization framework provides a platform for coupled dynamic analysis of wind turbines that can handle different models across different physics domains using a rigorous coupling scheme, allowing new model features to be easier to incorporate. This verification work yielded consistent results within the modeling considerations, which gives us confidence in the framework and its modules. We verified the capabilities of the framework to model different fixed-bottom offshore wind turbines against results from the code comparisons of the international OC3 and OC4 projects. The other codes from the various participants range from commercial software to research codes, and from stand-alone to aeroelastic codes coupled to finite-element software. A description of the capabilities and methods of these design codes can be found in Refs. 3 and 17. FAST v8 stands as an open-source tool with flexibility to include different modules to model the various physics domains for dynamics analysis and design of horizontal axis wind turbines.

As a first step in this work, we presented the results corresponding to a monopile substructure with the 5-MW NREL baseline wind turbine. Generally, we observed good agreement of local and global dynamics in a variety of load cases. Differences found among the OC3 project participants and between FAST v7 and FAST v8 can be related to the different modeling approaches. The main difference is the representation of the tower and monopile with four mode shapes in FAST v7, versus the modular representation in the FAST v8 framework, which couples the substructure (i.e., finite-element model, reduced via Craig-Bampton method) and the tower (i.e., mode shapes) with the rest of the wind turbine subsystems.

Tripod and jacket substructures coupled also to the 5-MW NREL baseline wind turbine (albeit with a different tower structure) were used to verify the capability to model the hydrodynamic loading and structural response of multimember substructures. HydroDyn calculates the wave kinematics and hydrodynamic loads, and SubDyn computes the dynamic response of the structure to hydrodynamic loads and wind and cyclic loads from the wind turbine on top. Here is a summary of our main observations from this work:

- The bandwidth of the coupled model should be considered carefully to achieve the desired computational speed and accuracy. Because the wind and wave excitation drop dramatically beyond 4 Hz; keeping only the lower modes and the quasi-static solution of the higher frequency modes of the substructure in SubDyn yields reasonable results at lower frequencies.

- In multimember substructures with large inclined members, as in the case of the tripod, axial loads dominate the response and are well represented by FAST v8. Shear forces that are very small compared to the ones in the axial direction and the components influenced by gravity and buoyancy show differences in FAST v8 compared to other codes. The main reason for this is that volume at the joints in FAST v8 is overestimated because overlapping of members is not taken into account.

- Loads on the substructure close to MSL reported by other codes using wave stretching models to resolve wave kinematics up to the instantaneous free surface showed a significantly larger amplitude than those from FAST v8, which only resolves the wave kinematics to MSL.

- Reaction loads at the substructure base showed that weight and overturning moment are well represented in FAST v8. This can be achieved with very few or none of the Craig-Bampton modes, using the static improvement method in SubDyn.

Verification and validation of analysis and design codes for wind turbines is an ongoing work. Some examples of future work in terms of FAST v8 development include linearization of the full system, nonlinear beam dynamics, calculation of overlapping volume in member joints, wave stretching, and tapered substructure members.

Acknowledgments

This work was performed at NREL and supported by the U.S. Department of Energy under Contract No. DE-AC36-08GO28308 with the National Renewable Energy Laboratory. Funding for the work was provided by the DOE Office of Energy Efficiency and Renewable Energy, Wind and Water Power Technologies Office.

References

[1] Passon, P., Kühn, M., Butterfield, S., Jonkman, J., Camp, T., and Larsen, T. J., "OC3–Benchmark Exercise of Aero-Elastic Offshore Wind Turbine Codes," *Journal of Physics: Conference Series*, Vol. 75, IOP Publishing, 2007, p. 012071.

[2] Nichols, J., et al., "Offshore Code Comparison Collaboration Within IEA Wind Annex XXIII: Phase III Results Regarding Tripod Support Structure Modeling," *47th AIAA Aerospace Sciences Meeting and Exhibit, 5–8 January 2008, Orlando, FL, AIAA Meeting Papers on Disc 14 (1)*, 2009.

[3] Popko, W., et al., "Offshore Code Comparison Collaboration Continuation (OC4), Phase I–Results of Coupled Simulations of an Offshore Wind Turbine with Jacket Support Structure," *Journal of Ocean and Wind Energy*, Vol. 1, 2014, pp. 1–11.

[4] Jonkman, J. M., and Buhl Jr, M. L., "FAST Users Guide," National Renewable Energy Laboratory, Golden, CO, 2005.

[5] Jonkman, J. M., "The New Modularization Framework for the FAST Wind Turbine CAE Tool," *51st AIAA Aerospace Sciences Meeting and 31st ASME Wind Energy Symposium*, Grapevine, TX, 2013.

[6] "NWTC Information Portal (FAST v8)." https://nwtc.nrel.gov/FAST8. Last modified 06 October 2014; [cited 14 October 2014.]

[7] Sprague, M., Jonkman, J., and Jonkman, B., "FAST Modular Wind Turbine CAE Tool: Nonmatching Spatial and Temporal Meshes," *SciTech2014 National Harbor, MD*, January 2014.

[8] "NWTC Information Portal (SubDyn)." https://nwtc.nrel.gov/SubDyn. Last modified 07 October 2014; [cited 10 November 2014].

[9] Song, H., Damiani, R., Robertson, A., Jonkman, J., et al., "A New Structural-Dynamics Module for Offshore Multimember Substructures Within the Wind Turbine Computer-Aided Engineering Tool FAST," *The Twenty-Third International Offshore and Polar Engineering Conference*, International Society of Offshore and Polar Engineers, Maui, HI, 2013.

[10] Damiani, R. R., Song, H., Robertson, A. N., and Jonkman, J. M., "Assessing the Importance of Nonlinearities in the Development of a Substructure Model for the Wind Turbine CAE Tool FAST," *ASME 2013 32nd International Conference on Ocean, Offshore and Arctic Engineering*, ASME, Washington, DC,2013, pp. V008T09A093–V008T09A093.

[11] "NWTC Information Portal (HydroDyn)." https://nwtc.nrel.gov/HydroDyn. Last modified 06 October 2014; [cited 10 November 2014].

[12] Song, H., et al., "Incorporation of Multi-Member Substructure Capabilities in FAST for Analysis of Offshore Wind Turbines," *Offshore Technology Conference, Houston, TX,* April, 2012.

[13] Jonkman, J. M., Butterfield, S., Musial, W., and Scott, G., "Definition of a 5-MW Reference Wind Turbine for Offshore System Development," National Renewable Energy Laboratory, Golden, CO, 2009.

[14] Jonkman, J. and Musial, W., "Offshore Code Comparison Collaboration (OC3) for IEA Task 23 Offshore Wind Technology and Deployment," NREL/TP-500-48191, National Renewable Energy Laboratory, Golden, CO, 2010.

[15] Vorpahl, F., et al., "Fully-Coupled Wind Turbine Simulation Including Substructuring of Support Structure Components: Influence of Newly Developed Modeling Approach on Fatigue Loads for an Offshore Wind Turbine on a Tripod Support Structure," *Proceedings of the Twenty-First International Offshore and Polar Engineering Conference,* Maui, HI, International Society of Offshore and Polar Engineers, 2011, pp. 284–290.

[16] Vorpahl, D.-I. F. and Popko, W., "Description of the Load Cases and Output Sensors to be Simulated in the OC4 Project under IEA Wind Annex 30," Fraunhofer Institute for Wind Energy and Energy System Technology IWES, Bremerhaven, Germany, 2013.

[17] Vorpahl, F., Strobel, M., Jonkman, J. M., Larsen, T. J., Passon, P., and Nichols, J., "Verification of Aero-Elastic Offshore Wind Turbine Design Codes Under IEA Wind Task XXIII," *Wind Energy*, Vol. 17, No. 4, 2014, pp. 519–547.